Environmental Science: Atmospheres

ROYAL SOCIETY OF CHEMISTRY

PAPER

View Article Online
View Journal | View Issue

Cite this: *Environ. Sci.: Atmos.*, 2022, **2**, 182

A dominant contribution to light absorption by methanol-insoluble brown carbon produced in the combustion of biomass fuels typically consumed in wildland fires in the United States†

Khairallah Atwi, Zezhen Cheng, ‡ Omar El Hajj, Charles Perrie and Rawad Saleh *

The light-absorption properties of brown carbon (BrC) are often estimated using offline, solvent-extraction methods. However, recent studies have found evidence of insoluble BrC species that are unaccounted for in solvent extraction. In this work, we produced carbonaceous aerosol particles from the combustion of three biomass fuels (pine needles, hickory twigs, and oak foliage). We utilized a combination of online and offline measurements and optical calculations to estimate the mass fractions and contribution to light absorption by methanol-soluble BrC (MSBrC), methanol-insoluble BrC (MIBrC), and elemental carbon (EC). Averaged over all experiments, the majority of the carbonaceous aerosol species were attributed to MSBrC (90% ± 5%), while MIBrC and EC constituted 9% ± 5% and 1% ± 0.5%, respectively. The BrC produced in all experiments was moderately absorbing, with an imaginary component of the refractive index (k) at 532 nm ranging between 0.01 and 0.05. However, the k values at 532 nm of the MSBrC (0.004 ± 0.002) and MIBrC (0.211 ± 0.113) fractions were separated by two orders of magnitude, with MSBrC categorized as weakly absorbing BrC and MIBrC as strongly absorbing BrC. Consequently, even though MSBrC constituted the majority of the aerosol mass, MIBrC had a dominant contribution to light absorption at 532 nm (72% ± 11%). The findings presented in this paper provide support for previous reports of the existence of strongly absorbing, methanol-insoluble BrC species and indicate that relying on methanol extraction to characterize BrC in biomass-burning emissions would severely underestimate its absorption.

Received 10th August 2021
Accepted 21st December 2021

DOI: 10.1039/d1ea00065a

rsc.li/esatmospheres

Environmental significance

Organic aerosol produced from biomass burning is an important player in the radiative balance in the atmosphere. However, there are major challenges associated with characterizing the optical properties of light-absorbing organic aerosol, or brown carbon, which hinder accurate representation of its interaction with solar radiation in climate calculations. Here, we show that conventional techniques that rely on extracting brown carbon in methanol to characterize its optical properties can severely underestimate brown carbon light absorption. Even though the methanol-insoluble fraction constituted less than 10% of the brown carbon mass on average in our experiments, it contributed more than 70% of the total mid-visible light absorption. Accounting for methanol-insoluble brown carbon will enhance the representation of biomass-burning aerosol in climate calculations.

Introduction

Combustion sources produce different species of light-absorbing particles that perturb the radiative balance in the atmosphere.[1] Black carbon (BC), the most absorbing of those species, is one of the three most potent contributors to radiative forcing, along with carbon dioxide and methane.[2] Other light-absorbing species, known as brown carbon (BrC),[3,4] absorb light less efficiently than BC, yet exert significant radiative forcing,[5–11] with estimates assigning it up to 50% of light absorption at short wavelengths and 25% of total radiative forcing by absorbing particles.[5,6]

The light-absorption properties of BrC, described by the imaginary component of the refractive index, k, vary greatly.[12] Values of k at mid-visible wavelengths of different BrC species have been reported between 10^{-4} and 10^{-1}, spanning several orders of magnitude.[13–18] At the same time, the wavelength dependence of BrC absorption is also highly variable, with stronger wavelength dependence exhibited by the less

Air Quality and Climate Research Laboratory, School of Environmental, Civil, Agricultural and Mechanical Engineering, University of Georgia, Athens, GA, USA. E-mail: rawad@uga.edu

† Electronic supplementary information (ESI) available. See DOI: 10.1039/d1ea00065a

‡ Current address: Pacific Northwest National Laboratory, Richland, WA, USA.

absorbing BrC.[13,14,19–23] While BrC was originally thought to be solely produced by low-temperature, smoldering biomass combustion, more recent works have identified BrC species emitted from higher-temperature biomass combustion[13,19–21,24] as well as the combustion of liquid fossil fuels.[18,22,25] In addition, the operational definitions of BrC have expanded to include strongly absorbing, non-volatile, and refractory species.[12,14,18,26]

Thus, the umbrella term BrC covers a range of organic species with widely varying light-absorption and physicochemical properties. This broad range of properties causes a large uncertainty associated with the effect of BrC on the radiative balance in the atmosphere.[12] In particular, the majority of climate models that represent BrC absorption use a singular set of parameters (*i.e.*, k values) to represent the various light-absorbing organic species due to the difficulty of including a more comprehensive representation. This can underestimate the direct radiative effect of BrC by skewing towards the less-absorbing species, partly due to a dated understanding of BrC that excludes absorption at longer wavelengths. An effective representation of BrC in climate models must thus reduce the complexity associated with representing thousands of species while, at the same time, effectively capture the relevant light-absorption and physicochemical properties.

In recent years, parameterizations and categorizations have been introduced to facilitate this outcome. Saleh *et al.* (2014)[19] showed that light-absorption properties of BrC emitted from biomass burning can be parameterized as a function of the emissions' relative BC and OA content. Those parameterizations have been implemented in some models, yielding a better agreement between model predictions and observations.[8] More recent classifications of BrC have also been proposed based on their physicochemical properties. Corbin *et al.* (2019)[18] divided BrC into soluble BrC and tar BrC, defined by their solubility or insolubility, respectively, in any of the commonly used solvents such as water, methanol, and acetone. Corbin *et al.*'s categorization of BrC further includes physicochemical properties characteristic of each category, such as light-absorption properties, volatility, and molecular size. Hettiyadura *et al.* (2021)[23] reported the existence of BrC chromophores, containing nonpolar and less-polar PAHs, that were found only in an "oily" fraction of tar condensates. Those oil-specific compounds were overall less volatile and more viscous than other BrC components. Saleh (2020)[12] presented a classification based on light-absorption properties, dividing BrC into 4 bins spanning the 4 orders of magnitude covered by mid-visible k values of BrC reported in the literature. Saleh's light-absorption-based BrC classification also highlights that more absorbing BrC species tend to be less volatile and less soluble in water and organic solvents, and to have larger molecular sizes.

The distinction drawn by Corbin *et al.*[18] between soluble and insoluble BrC can be further extended to distinguish soluble species of BrC. Indeed, numerous studies have found that water-soluble BrC is less absorbing than methanol-soluble BrC.[27–29] Further, Cheng *et al.* (2020)[17] showed that some BrC produced from the combustion of single-molecule fuels was insoluble in methanol but soluble in dichloromethane (DCM), with the DCM-soluble species being more light absorbing than the methanol-soluble species. Cheng *et al.*[17] also found that a significant fraction of some BrC samples could be insoluble in both. Those insoluble BrC species create a disagreement between the light-absorption properties retrieved *via* solvent-extraction methods and those retrieved in online measurements. In fact, Shetty *et al.* (2019)[30] found that the light-absorption properties of biomass-burning particles retrieved using solvent-extraction methods and those retrieved from online measurements could differ by up to a factor of 10, with the discrepancy increasing with increasing elemental carbon (EC) content. Higher EC content is correlated with stronger light absorption by biomass-burning BrC,[13,19] thus the findings of Shetty *et al.*[30] are consistent with the aforementioned association between light absorption and solubility in water and organic solvents.

In this paper, we present further evidence of biomass-burning BrC that is insoluble in methanol. We use a combination of online and offline measurements to apportion the biomass-burning BrC into methanol-soluble and methanol-insoluble fractions and retrieve the light-absorption properties of each fraction. Doing so, we show that even though the majority of the BrC was methanol-soluble, the light absorption was dominated by the methanol-insoluble BrC.

Methods

Experimental procedure

We burnt dead pine needles, hickory twigs, and dead oak foliage inside a 7.5 m^3 environmental chamber. These fuels are commonly consumed in wildfires and prescribed burns in the Southeastern United States.[31,32] The fuels were dried inside an oven at 60 °C for 24 hours to reduce their moisture content. Approximately 50 g of each fuel was burned inside an environmental chamber. The fuels were allowed to burn inside the chamber for tens of seconds up to a minute. We then performed online measurements and collected filter samples for offline measurements over a period of several hours.

A scanning mobility particle sizer (SMPS, TSI 3882) continuously measured the particle size distribution in the range of 10–500 nm. We used a photoacoustic spectrometer (Multi-PAS III)[33] to measure the absorption coefficient (b_{abs}, Mm^{-1}) of the aerosol at 3 wavelengths: 422 nm, 532 nm, and 782 nm. As described in the following sections, these online measurements were used to retrieve the aerosol light-absorption properties.

We collected particles on two filter trains at a flow rate of 5 SLPM for offline analysis. One consisted of a sole 47 mm Quartz (Q) filter (Pall Inc., Tissuquartz 2500), the other of a 47 mm Teflon (PTFE) filter (0.2 microns, Sterlitech Corporation, PTU024750) followed by a Quartz behind Teflon filter (QBT). We targeted a total particle mass loading of 300 μg on the Quartz and Teflon filters, estimated from the sampling flowrate and total particle mass concentration obtained from SMPS measurements. Depending on the particle concentration in the environmental chamber, we collected the filter samples for several hours until the target loading was approximately reached. The Quartz and QBT filters were used to determine the mass fractions of methanol-soluble BrC (MSBrC), methanol-

insoluble BrC (MIBrC), and EC, and the PTFE filter was used to determine the light-absorption properties of MSBrC, as elaborated in the subsequent sections.

Mass apportionment

The procedure to apportion the particle mass into fractions of MSBrC, MIBrC, and EC is illustrated in Fig. 1. We immersed a 1.5 cm^2 punch of the Quartz filter in 3 ml of methanol for 24 hours in a process of passive extraction, *i.e.*, without sonication. This process minimizes the physical extraction of methanol-insoluble species from the Quartz filter, while also preserving the integrity of the filter for the subsequent analysis.[30,34] We performed the extraction in the dark at 4 °C in order to minimize photolysis-induced reactions that could lead to destruction of BrC chromophores[35] (photobleaching). After 24 hours, the Quartz punch was removed and dried using a stream of clean, dry air. We then used an organic carbon – elemental carbon (OCEC) analyzer (Sunset Laboratory Inc, Portland, OR, USA, Model 5 L) running the NIOSH-870 protocol (see ESI Table S1†) to determine the residual total carbon (TC) mass on the filter punch after extraction ($TC_{Q,residual}$). As further elaborated below, $TC_{Q,residual}$ corresponds to TC of the methanol-insoluble species, including both MIBrC and EC:

$$TC_{Q,residual} = OC_{MIBrC} + EC \quad (1)$$

Here, OC_{MIBrC} and EC were obtained from the OCEC analyzer measurements of the residual carbonaceous material on the Quartz punch after extraction. The OCEC analyzer divides the analyte into OC and EC depending on the temperature and conditions at which they desorb during the analysis. It also identifies pyrolyzed OC, which corresponds to organic species that become pyrolyzed during the initial heating phase, resisting volatilization in the oxygen-deficient phase and appearing instead with the EC.[36,37] In eqn (1), OC_{MIBrC} includes both the non-pyrolyzed and the pyrolyzed OC reported by the OCEC analyzer. An implicit assumption in eqn (1) is that all the carbon in MIBrC is detected as OC in the OCEC analyzer. In reality, it is possible that some strongly absorbing, refractory BrC is mistakenly classified as EC by thermal-optical measurements.[18,22,38] Thus, OC_{MIBrC} could be underestimated and EC overestimated in the analysis.

In order to determine the methanol-soluble OC (OC_{MSBrC}) fraction, we used the same OCEC analysis procedure to determine the TC mass on an unextracted Quartz filter punch (TC_Q) and on a QBT filter punch (TC_{QBT}). Since the QBT filter only collected adsorbed vapor species, the difference between TC_Q and TC_{QBT} corresponds to the TC in the particle phase,[39] including MSBrC, MIBrC, and EC:

$$TC_Q - TC_{QBT} = OC_{MSBrC} + OC_{MIBrC} + EC \quad (2)$$

Then, OC_{MSBrC} can be obtained from eqn (1) and (2) as:

$$OC_{MSBrC} = (TC_Q - TC_{QBT}) - TC_{Q,residual} \quad (3)$$

We converted OC_{MSBrC} and OC_{MIBrC} to organic-mass basis (OM_{MSBrC} and OM_{MIBrC}) assuming OM/OC of 1.8, which is typical for biomass-combustion emissions.[40–42] As shown in Table S2 in the ESI,† assuming OM/OC of 1.5–2 did not have a significant effect on the retrieved light-absorption properties. The fractions of MSBrC, MIBrC, and EC in the particles were then obtained as:

$$f_{MSBrC} = OM_{MSBrC}/TM;\ f_{MIBrC} = OM_{MIBrC}/TM;\ f_{EC} = EC/TM \quad (4)$$

Where TM is the total mass of carbonaceous species:

$$TM = OM_{MSBrC} + OM_{MIBrC} + EC \quad (5)$$

Retrieving aerosol light-absorption properties

We retrieved the imaginary component of the refractive index of the BrC aerosol ($k_{BrC,aerosol}$) at 422 nm and 532 nm using optical closure.[13,19,43,44] In brief, we used Mie calculations to constrain

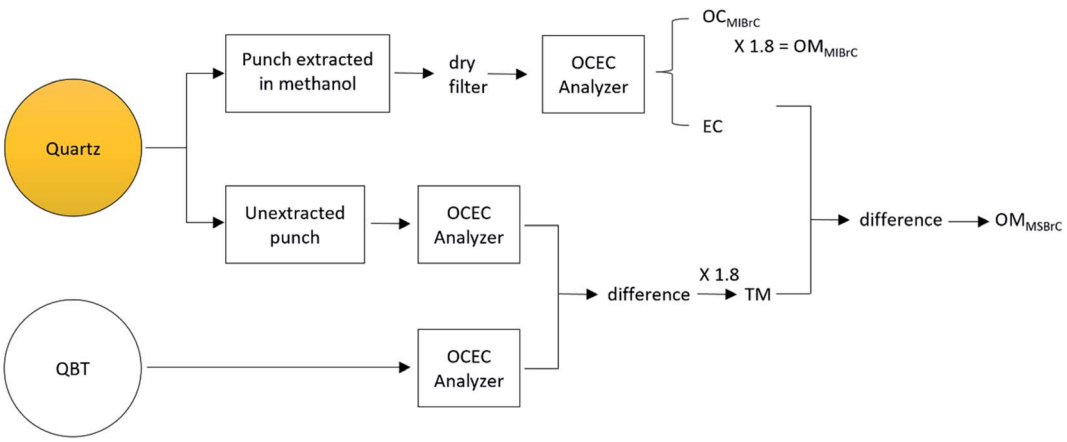

Fig. 1 Flowchart summarizing the procedure for apportioning the carbonaceous particle mass into methanol-soluble BrC (MSBrC), methanol-insoluble BrC (MIBrC), and EC (see eqn (1)–(5)).

the $k_{BrC,aerosol}$ that, coupled with measured particle size distributions, best reproduced the measured b_{abs} at that wavelength. We calculated the wavelength dependence, $w_{BrC,aerosol}$, assuming that $k_{BrC,aerosol}$ exhibits a power-law dependence on wavelength:

$$w_{BrC,aerosol} = \log(k_{422,BrC,aerosol}/k_{532,BrC,aerosol})/\log(532/422) \quad (6)$$

The Mie calculations assumed a BrC real component of the refractive index equal to 1.6.[12] To account for absorption by EC, we applied several assumptions. First, we assumed that EC and BrC were externally mixed. We also assumed that the EC particles were spherical (which is inherent in Mie calculations) and that their size distribution had the same shape as that of BrC. Therefore, the size distributions measured by the SMPS were split between EC and BrC based on the EC/OM values obtained from the OCEC analyzer measurements. Finally, we used an EC complex refractive index of $1.85 + 0.71i$.[45] We note that because the EC fraction was small in these experiments (EC/OC < 0.05), these simplifying assumptions had a small effect on the retrieved $k_{BrC,aerosol}$ as discussed in Section S2 in the ESI.†

Light-absorption apportionment

As summarized in Fig. 2, we employed a combination of online and offline measurements and Mie calculations to retrieve the imaginary component of the refractive indices of methanol-soluble BrC (k_{MSBrC}) and methanol-insoluble BrC (k_{MIBrC}). First, we used the particles collected on the PTFE filters to determine the light-absorption properties of MSBrC following the procedure of Cheng *et al.* (2020).[17] For the extraction of the PTFE filters, we immersed each filter in 5 ml of methanol inside a glass vial and sonicated for 15 minutes. In preliminary experiments, we confirmed that sonication for longer times (up to 30 minutes) had no observable effect on extraction efficiency. Unlike with the passive extraction used with the Quartz filters, sonication can physically extract some of the methanol-insoluble species. To remove the methanol-insoluble particles from the methanol solution, we filtered the methanol extracts through 13 mm PTFE (0.2 microns, Sterlitech Corporation, PTU021350) using a glass vial with a metal luer lock tip.

We measured the MSBrC concentration in the solutions using the OCEC analyzer. To do so, we pipetted 300 μl onto 1.5 cm^2 punches of prebaked Quartz filters and dried the filters using a stream of clean, dry air. Because methanol is relatively volatile, it evaporates rapidly under the stream of air, leaving behind the BrC. We then retrieved the total carbon mass on the punch running the NIOSH-870 protocol on the OCEC analyzer. We used the measured mass to estimate the BrC concentration in the solutions, C_{MSBrC}. As before, we assumed OM/OC = 1.8.

We used a UV-vis Spectrophotometer (Agilent, Cary 60) to measure the UV-vis absorbance of the extracts in the 200–800 nm range at a 1 nm resolution. We then converted the measured absorbance to light-absorption properties of MSBrC using the relation between k_{MSBrC} and the absorption coefficient (α, cm^{-1}):

$$k_{MSBrC,\lambda} = \lambda\alpha(\lambda)/4\pi \quad (7)$$

Here, α is calculated from the UV-vis measurements using

$$\alpha(\lambda) = \ln(10)A(\lambda)\rho/(C_{MSBrC}L) \quad (8)$$

where A is the measured absorbance, ρ is the density of the extracts (assumed to be 1.2 g cm^{-3}), L (1 cm) is the optical path length, and C_{MSBrC} is the concentration of MSBrC in the solution. Although the absorption coefficients α and b_{abs} have similar units ($length^{-1}$), they express different physical quantities. b_{abs} represents the total absorption cross section of the aerosol per unit volume of air and thus depends on the aerosol concentration and size distribution, whereas α is a material property that is directly related to k (eqn (7)).

We retrieved k_{MIBrC} based on the assumption that MIBrC and MSBrC were well-mixed in the BrC aerosol and that $k_{BrC,aerosol}$ is a volume-weighted average of k_{MSBrC} and k_{MIBrC}. Therefore:

$$k_{MIBrC} = (k_{BrC,aerosol} - k_{MSBrC}f_{MSBrC}/(f_{MSBrC} + f_{MIBrC})) \times (f_{MSBrC} + f_{MIBrC})/f_{MIBrC} \quad (9)$$

where, k_{MSBrC} is obtained from the UV-vis measurements, $k_{BrC,aerosol}$ is obtained from the optical closure analysis, and the fractions (f_{MSBrC} and f_{MIBrC}) are obtained from the mass apportionment analysis.

We also quantified the fractional contribution to light absorption by MSBrC, MIBrC, and EC. The fractional contribution by EC was calculated as:

$$X_{abs,EC} = b_{abs,EC}/b_{abs} \quad (10)$$

where $b_{abs,EC}$ is the absorption coefficient of the EC particles, obtained using Mie calculations and b_{abs} is the total aerosol

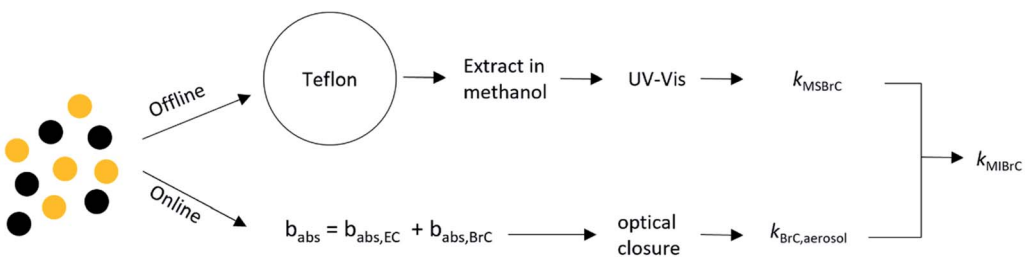

Fig. 2 Flowchart showing the light-absorption apportionment procedure (see eqn (7)–(9)).

absorption coefficient measured using the Multi-PAS III. The contributions to absorption by MSBrC and MIBrC were then calculated as:

$$X_{\mathrm{abs,MSBrC}} = (1 - X_{\mathrm{abs,EC}})(k_{\mathrm{MSBrC}} f_{\mathrm{MSBrC}}/(f_{\mathrm{MSBrC}} + f_{\mathrm{MIBrC}}))/k_{\mathrm{BrC,aerosol}} \quad (11)$$

$$X_{\mathrm{abs,MIBrC}} = (1 - X_{\mathrm{abs,EC}})(k_{\mathrm{MIBrC}} f_{\mathrm{MIBrC}}/(f_{\mathrm{MSBrC}} + f_{\mathrm{MIBrC}}))/k_{\mathrm{BrC,aerosol}} \quad (12)$$

The uncertainty associated with these calculations is discussed in Section S1 in the ESI.†

Results

Brown carbon aerosol light-absorption properties

Fig. 3 shows the light-absorption properties (k_{550} and w) of the BrC aerosol plotted against the EC/OM ratios retrieved from the OCEC analyzer. We note that here we use the term 'BrC aerosol' to refer to the whole BrC and to indicate that its light-absorption properties were obtained from online measurements in the aerosol phase followed by the subtraction of EC absorption, as described earlier. The individual data points shown correspond to the combustion experiments we conducted with each of the three fuels. On the same figures, we show the parameterizations of k_{550} and w *versus* EC/OM (or, equivalently, BC/OA) derived by Saleh *et al.* (2014),[19] based on both internally mixed and externally mixed BC assumptions. For both k_{550} and w, our data agree with the trends of correlation between the light-absorption properties and EC/OM, with k_{550} increasing and w decreasing with increasing EC content. The inverse relation between k and w has also been repeatedly established previously for BrC.[13,21,46] Notably, the data points from the different combustion experiments follow a similar trend, with no apparent dependence on fuel type. This indicates that the difference in the light-absorption properties of BrC produced in different combustion scenarios is primarily dictated by the different combustion conditions rather than fuel type.[14]

Both k_{550} and w values obtained in this study are generally larger than those predicted by the Saleh *et al.*[19] parameterizations. This could be due to true variability, but is also likely due to discrepancies in aerosol light-absorption measurements between the two studies. BrC parameterizations derived from biomass-burning measurements usually involve significant spread in the data points,[13,19,47] and while they usually exhibit similar trends, there are large differences between them.[12] Because of the relatively small number of data points and limited range of EC/OM in this study, we elect not to report a mathematical fit.

Light-absorption properties of the methanol-soluble and methanol-insoluble brown carbon

Fig. 4 shows the imaginary component of the refractive indices of the MSBrC and MIBrC fractions (k_{MSBrC} and k_{MIBrC}) at 422 nm and 532 nm, plotted against $k_{\mathrm{BrC,aerosol}}$. The figure shows that k_{MSBrC} and k_{MIBrC} are clustered in different ranges. $k_{\mathrm{MSBrC,422}}$ and $k_{\mathrm{MSBrC,532}}$ had average values of 0.015 ± 0.003 and 0.004 ± 0.002, respectively, while $k_{\mathrm{MIBrC,422}}$ and $k_{\mathrm{MIBrC,532}}$ had average values of 0.308 ± 0.161 and 0.211 ± 0.113, respectively. At both wavelengths, MSBrC had a smaller k than the BrC aerosol, while MIBrC had a larger k than the BrC aerosol. In-line with previous reports,[17,18,25,30] an important implication of these findings is that relying on methanol extraction can severely underestimate BrC absorption. Furthermore, as $k_{\mathrm{BrC,aerosol}}$ increases, k_{MSBrC} is relatively capped, which further indicates that methanol extraction becomes less effective in capturing the light-absorption properties of the BrC particles as a whole as they become more absorbing.[17]

In Fig. 5, we show the light-absorption properties (k_{550} *vs.* w) of the BrC aerosol and the MSBrC and MIBrC fractions retrieved

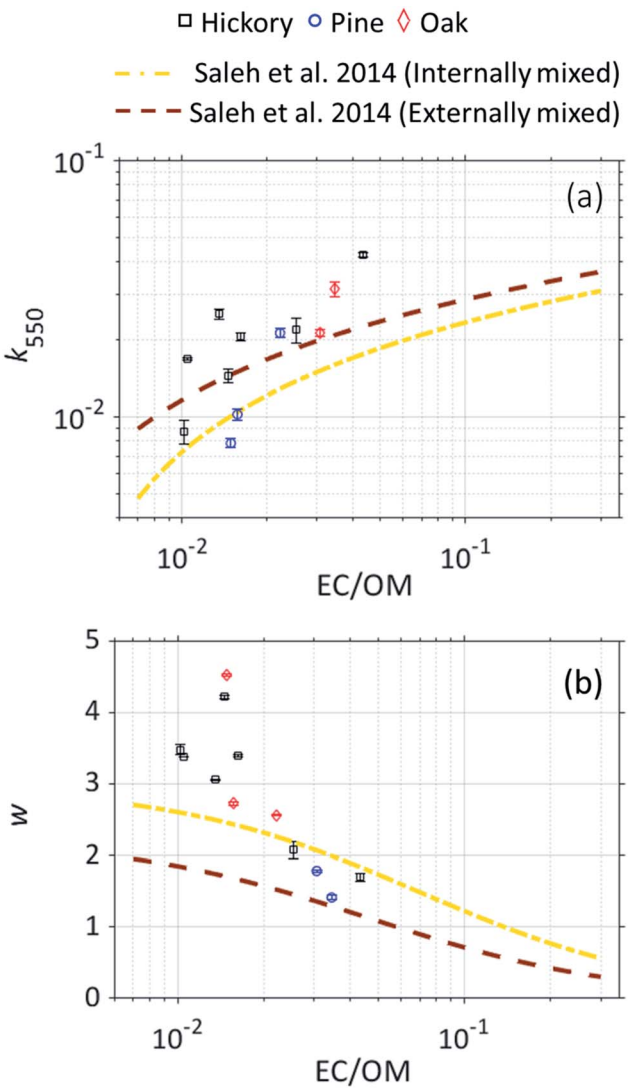

Fig. 3 Light-absorption properties of the BrC aerosol, retrieved using optical closure, as a function of the EC/OM ratio, retrieved from the OCEC analyzer assuming OM/OC = 1.8. (a) The imaginary component of the refractive index at 550 nm (k_{550}) *versus* EC/OM. (b) The wavelength dependence of the imaginary component of the refractive index (w) *versus* EC/OM. Also shown are the parameterizations of Saleh *et al.* (2014)[19] with the assumption of internally mixed and externally mixed BC. Error bars represent uncertainty, calculated as described in the ESI.†

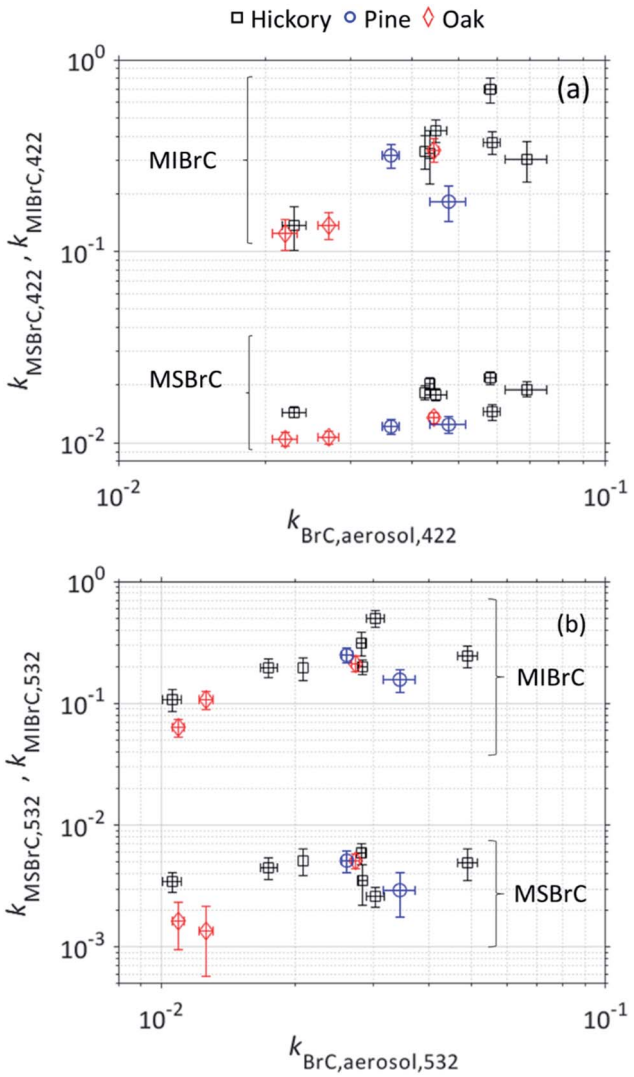

Fig. 4 The imaginary component of the refractive index (k) for the methanol-soluble BrC (MSBrC) and the methanol-insoluble BrC (MIBrC), retrieved from UV-Vis measurements and optical closure, respectively, plotted against k of the BrC aerosol at (a) $\lambda = 422$ nm and (b) $\lambda = 532$ nm. Error bars represent uncertainty, calculated as described in the ESI.† Numerical values of each data point are given in Table S2 in the ESI.†

in this study. In the backdrop, we show the BrC categories proposed by Saleh (2020)[12] along with literature values of biomass-burning BrC k_{550} *vs.* w retrieved based on methanol extraction (*i.e.*, equivalent to MSBrC in this study). The BrC aerosol produced in this study falls within the moderately absorbing BrC category (M-BrC). However, the fractions that compose it, namely MSBrC and MIBrC, are divided between the weakly absorbing BrC category (W-BrC) and the strongly absorbing category (S-BrC), respectively. The mean MIBrC k_{550} from all experiments is 2 orders of magnitude larger than MSBrC k_{550} ($k_{MIBrC,550} = 0.211 \pm 0.113$; $k_{MSBrC,550} = 0.004 \pm 0.002$), while MSBrC exhibited a much stronger wavelength dependence ($w_{MIBrC} = 1.7 \pm 1.1$; $w_{MSBrC} = 6.3 \pm 1.7$). The light-absorption properties of MSBrC obtained from our experiments are consistent with those reported for biomass-burning BrC in other works that relied on methanol extraction,[21,29,48–51] all of which fall within W-BrC. Those studies investigated emissions from a wide range of biomass fuels, including wood for residential heating/cooking,[21] agricultural waste[48] (corn stalk), as well as ambient aerosol with strong contributions from residential and agricultural burning.[49–51] This indicates that our finding that MSBrC falls within the W-BrC category extends beyond the fuel types investigated in our experiments. Furthermore, previous studies retrieved BrC light-absorption properties from measurements in the aerosol phase, including in emissions from residential wood burning[20] and agricultural burning[19] (rice straw, hay). These studies reported k_{BrC} values that fall within the M-BrC category,[12] and are typically larger than the values from the aforementioned studies that relied on methanol extraction. This suggests that MIBrC is possibly important in emissions from these fuel types.

The stronger light absorption of MIBrC compared to MSBrC reported here and in other works[17,18,25] confirms that MSBrC cannot be used to represent the light-absorption properties of BrC aerosols as a whole. The methanol-insoluble fraction must be accounted for in order to arrive at an accurate representation of absorption by BrC. The light-absorption properties of the MIBrC in our experiments span a similar range to that suggested by Corbin *et al.* (2019)[18] for marine-engine exhaust, as well as other reports of strongly absorbing BrC that have been referred to using different terminologies, including refractory BrC,[14] intermediate absorber (between BrC and BC),[52] BrC associated with extremely low volatility organic compounds (ELVOCs),[19] and brown carbon spheres.[53]

Mass fractions and contribution to absorption

Fig. 6 shows the mass fractions of MSBrC (f_{MSBrC}), MIBrC (f_{MIBrC}), and EC (f_{EC}) in the carbonaceous aerosol, averaged over all the combustion experiments. MSBrC constituted by far the largest fraction (90% ± 5%), while MIBrC and EC constituted 9% ± 5% and 1% ± 0.5%, respectively. This is consistent with previous studies that have reported methanol extraction efficiencies of >90%.[29,48] Indeed, these high extraction efficiencies by methanol have led those studies to assume that methanol effectively extracts all the organics in biomass-burning particle emissions. While this assumption is justified when the purpose is to study the chemical composition of the OA (*e.g.*, to investigate OA formation pathways in biomass burning), it is not when the purpose is to quantify BrC light absorption.

Also shown in Fig. 6 are the estimated contributions to absorption by each of the MSBrC, MIBrC, and EC fractions, averaged over all experiments. Despite constituting the majority of the particles by mass, the MSBrC contributed 35% ± 11% and 16% ± 7% of the total absorption at 422 nm and 532 nm, respectively. In contrast, the MIBrC contributed 60% ± 11% and 72% ± 10% at 422 nm and 532 nm, respectively, and the EC fraction contributed 5% ± 3% and 12% ± 5% at 422 nm and 532 nm, respectively. It is worth noting that the relative differences between the contributions to absorption at 422 nm and 532 nm between MSBrC, MIBrC, and EC is a reflection of the

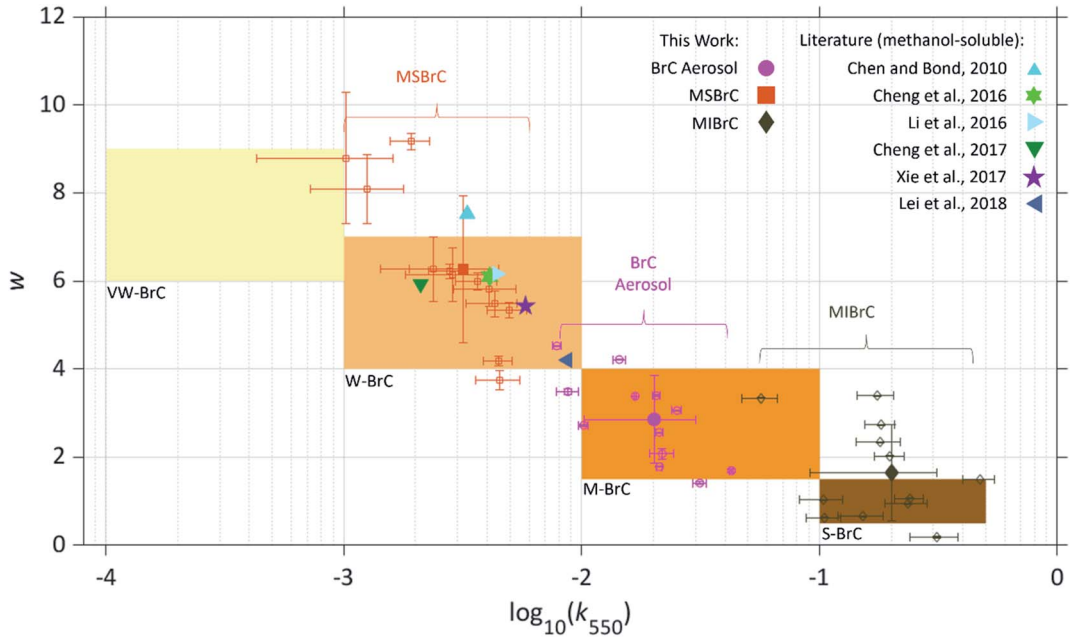

Fig. 5 Light-absorption properties of the BrC aerosol and the MSBrC and MIBrC fractions produced in this work, shown in $\log_{10}(k_{550})$ – w space. The shaded rectangles represent the BrC categories suggested by Saleh (2020).[12] Open circles, squares, and rhombi represent individual data points from each experiments and filled markers represent the average values retrieved for the categories of BrC aerosol, MSBrC, and MIBrC. To avoid cluttering, we did not include different markers for each fuel type in this figure. The figure also includes the average values of biomass-burning k_{550} *vs.* w reported in or calculated from previous studies that utilized methanol extraction.[24,29,48–51] Error bars represent uncertainty, calculated as described in the ESI.†

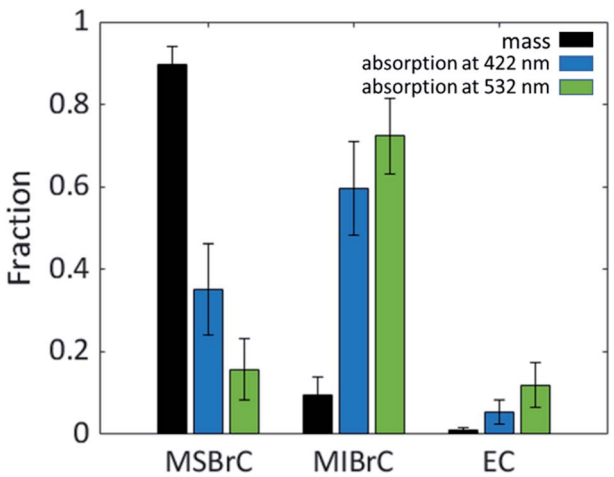

Fig. 6 Mass fractions of MSBrC, MIBrC, and EC averaged over all combustion experiments and their corresponding fractional contribution to total aerosol absorption at 422 nm and 532 nm. Error bars represent uncertainty, calculated as described in the ESI.†

differences in the wavelength dependence of their absorption. As shown in Fig. 5, w_{MSBrC} and w_{MIBrC} were 6.3 ± 1.7 and 1.7 ± 1.1, respectively, while w_{EC} was assumed to be zero.

Due to the limited number of experiments in this study, we were not able to investigate the source of variability in the relative abundance of MSBrC and MIBrC across experiments. Following from previous reports on BrC absorption being correlated with combustion conditions,[13,14,19] we expect that combustion conditions will also dictate the relative abundance of MSBrC and MIBrC. Specifically, we expect that the MIBrC fraction would be relatively small in smoldering combustion and would increase as combustion conditions become more flaming, leading to an overall increase in BrC absorption.

Importantly, even though MIBrC constitutes an order-of-magnitude smaller fraction of the carbonaceous aerosol than MSBrC, it contributes a dominant fraction of the total absorption. These findings are consistent with previous reports of a dominant contribution to absorption by insoluble BrC produced from heavy fuel oil combustion[18,25] and indicate that methanol-extraction techniques are inadequate at quantifying light absorption by biomass-burning BrC. In addition to its association with differences in light-absorption properties, solubility in methanol is also expected to be associated with other physicochemical properties, including volatility and molecular size.[14,18] Furthermore, larger molecular size BrC species have been shown to be more resistant to decay in absorption due to photobleaching upon aging in the atmosphere.[54] Consequently, in addition to MIBrC being more light-absorbing than MSBrC, it is also expected to be less volatile, possibly less susceptible to photobleaching, and therefore have a longer lifetime in the atmosphere.

Conclusions

In this work, we report the existence of a methanol-insoluble BrC (MIBrC) fraction produced in biomass combustion that is significantly more light absorbing than the methanol-soluble

BrC (MSBrC) fraction. These findings contribute to the growing body of literature on the association between solubility and the light-absorption properties of BrC produced in biomass combustion,[30] as well as controlled combustion of single-molecule fuels[17] and marine engines.[18,25] In concordance with previous studies,[29,48] methanol was efficient at extracting the organic matter produced in our biomass-burning experiment, where MSBrC constituted 90% ± 5% of the total carbonaceous species. However, considering this high methanol extraction efficiency as an indication that MSBrC is representative of the overall BrC is misleading. Our results show that relying on methanol extraction to constrain the light-absorption properties of biomass-burning BrC results in a severe misrepresentation of these properties, leading to an order-of-magnitude underestimation of BrC light absorption at mid-visible wavelengths.

Author contributions

Khairallah Atwi: methodology, formal analysis, investigation, data curation, validation, visualization, writing – original draft, writing – review & editing. Zezhen Cheng: methodology, writing – original draft. Omar El Hajj: investigation, writing – original draft. Charles Perrie: investigation, writing – original draft. Rawad Saleh: conceptualization, methodology, writing – original draft, writing – review & editing, supervision, project administration, funding acquisition.

Conflicts of interest

There are no conflicts to declare.

Acknowledgements

Financial support was provided by the National Science Foundation, Division of Atmospheric and Geospace Sciences (AGS-1748080).

Notes and references

1 T. C. Bond, S. J. Doherty, D. Fahey, P. Forster, T. Berntsen, B. DeAngelo, M. Flanner, S. Ghan, B. Kärcher and D. Koch, Bounding the role of black carbon in the climate system: A scientific assessment, *J. Geophys. Res.: Atmos.*, 2013, **118**, 5380–5552.

2 R. K. Pachauri, M. R. Allen, V. R. Barros, J. Broome, W. Cramer, R. Christ, J. A. Church, L. Clarke, Q. Dahe and P. Dasgupta, *Climate Change 2014: Synthesis Report. Contribution of Working Groups I, II and III to the Fifth Assessment Report of the Intergovernmental Panel on Climate Change*, IPCC, 2014.

3 A. Laskin, J. Laskin and S. A. Nizkorodov, Chemistry of atmospheric brown carbon, *Chem. Rev.*, 2015, **115**, 4335–4382.

4 M. Andreae and A. Gelencsér, Black carbon or brown carbon? The nature of light-absorbing carbonaceous aerosols, *Atmos. Chem. Phys.*, 2006, **6**, 3131–3148.

5 Y. Zhang, H. Forrister, J. Liu, J. Dibb, B. Anderson, J. P. Schwarz, A. E. Perring, J. L. Jimenez, P. Campuzano-Jost and Y. Wang, Top-of-atmosphere radiative forcing affected by brown carbon in the upper troposphere, *Nat. Geosci.*, 2017, **10**, 486–489.

6 X. Wang, C. Heald, D. Ridley, J. Schwarz, J. Spackman, A. Perring, H. Coe, D. Liu and A. Clarke, *Exploiting Simultaneous Observational Constraints on Mass and Absorption to Estimate the Global Direct Radiative Forcing of Black Carbon and Brown Carbon*, 2014.

7 Y. Feng, V. Ramanathan and V. R. Kotamarthi, Brown carbon: a significant atmospheric absorber of solar radiation?, *Atmos. Chem. Phys.*, 2013, **13**, 8607–8621.

8 H. Brown, X. Liu, Y. Feng, Y. Jiang, M. Wu, Z. Lu, C. Wu, S. Murphy and R. Pokhrel, *Radiative Effect and Climate Impacts of Brown Carbon with the Community Atmosphere Model (CAM5), Report 1680-7375*, Lawrence Berkeley National Laboratory (LBNL), Berkeley, CA (United States), 2018.

9 R. Saleh, M. Marks, J. Heo, P. J. Adams, N. M. Donahue and A. L. Robinson, Contribution of brown carbon and lensing to the direct radiative effect of carbonaceous aerosols from biomass and biofuel burning emissions, *J. Geophys. Res.: Atmos.*, 2015, **120**, 10285–10296.

10 R. J. Park, M. J. Kim, J. I. Jeong, D. Youn and S. Kim, A contribution of brown carbon aerosol to the aerosol light absorption and its radiative forcing in East Asia, *Atmos. Environ.*, 2010, **44**, 1414–1421.

11 M. Z. Jacobson, Effects of biomass burning on climate, accounting for heat and moisture fluxes, black and brown carbon, and cloud absorption effects, *J. Geophys. Res.: Atmos.*, 2014, **119**, 8980–9002.

12 R. Saleh, From Measurements to Models: Toward Accurate Representation of Brown Carbon in Climate Calculations, *Curr. Pollut. Rep.*, 2020, 1–15.

13 C. D. McClure, C. Y. Lim, D. H. Hagan, J. H. Kroll and C. D. Cappa, Biomass-burning-derived particles from a wide variety of fuels–Part 1: Properties of primary particles, *Atmos. Chem. Phys.*, 2020, **20**, 1531–1547.

14 R. Saleh, Z. Cheng and K. Atwi, The brown–black continuum of light-absorbing combustion aerosols, *Environ. Sci. Technol. Lett.*, 2018, **5**, 508–513.

15 A. T. Lambe, C. D. Cappa, P. Massoli, T. B. Onasch, S. D. Forestieri, A. T. Martin, M. J. Cummings, D. R. Croasdale, W. H. Brune and D. R. Worsnop, Relationship between oxidation level and optical properties of secondary organic aerosol, *Environ. Sci. Technol.*, 2013, **47**, 6349–6357.

16 K. M. Updyke, T. B. Nguyen and S. A. Nizkorodov, Formation of brown carbon via reactions of ammonia with secondary organic aerosols from biogenic and anthropogenic precursors, *Atmos. Environ.*, 2012, **63**, 22–31.

17 Z. Cheng, K. Atwi, O. E. Hajj, I. Ijeli, D. A. Fischer, G. Smith and R. Saleh, Discrepancies Between Brown Carbon Light-absorption Properties Retrieved from Online and Offline Measurements, *Aerosol Sci. Technol.*, 2020, 1–15.

18 J. C. Corbin, H. Czech, D. Massabò, F. B. de Mongeot, G. Jakobi, F. Liu, P. Lobo, C. Mennucci, A. A. Mensah and J. Orasche, Infrared-absorbing carbonaceous tar can dominate light absorption by marine-engine exhaust, *npj Clim. Atmos. Sci.*, 2019, **2**, 1–10.

19 R. Saleh, E. S. Robinson, D. S. Tkacik, A. T. Ahern, S. Liu, A. C. Aiken, R. C. Sullivan, A. A. Presto, M. K. Dubey and R. J. Yokelson, Brownness of organics in aerosols from biomass burning linked to their black carbon content, *Nat. Geosci.*, 2014, **7**, 647.

20 N. K. Kumar, J. C. Corbin, E. A. Bruns, D. Massabó, J. G. Slowik, L. Drinovec, G. Močnik, P. Prati, A. Vlachou and U. Baltensperger, Production of particulate brown carbon during atmospheric aging of residential wood-burning emissions, *Atmos. Chem. Phys.*, 2018, **18**, 17843–17861.

21 M. Xie, G. Shen, A. L. Holder, M. D. Hays and J. J. Jetter, Light absorption of organic carbon emitted from burning wood, charcoal, and kerosene in household cookstoves, *Environ. Pollut.*, 2018, **240**, 60–67.

22 Z. Z. Cheng, K. Atwi, T. Onyima and R. Saleh, Investigating the dependence of light-absorption properties of combustion carbonaceous aerosols on combustion conditions, *Aerosol Sci. Technol.*, 2019, **53**, 419–434.

23 A. P. S. Hettiyadura, V. Garcia, C. Li, C. P. West, J. Tomlin, Q. He, Y. Rudich and A. Laskin, Chemical Composition and Molecular-Specific Optical Properties of Atmospheric Brown Carbon Associated with Biomass Burning, *Environ. Sci. Technol.*, 2021, **55**, 2511–2521.

24 M. Xie, M. D. Hays and A. L. Holder, Light-absorbing organic carbon from prescribed and laboratory biomass burning and gasoline vehicle emissions, *Sci. Rep.*, 2017, **7**, 1–9.

25 Z. Bai, L. Zhang, Y. Cheng, W. Zhang, J. Mao, H. Chen, L. Li, L. Wang and J. Chen, Water/Methanol-Insoluble Brown Carbon Can Dominate Aerosol-Enhanced Light Absorption in Port Cities, *Environ. Sci. Technol.*, 2020, **54**, 14889–14898.

26 N. Shetty, P. Beeler, T. Paik, F. J. Brechtel and R. K. Chakrabarty, Bias in Quantification of Light Absorption Enhancement of Black Carbon Aerosol Coated with Low Volatility Brown Carbon, *Aerosol Sci. Technol.*, 2021, 1–16.

27 R.-J. Huang, L. Yang, J. Shen, W. Yuan, Y. Gong, J. Guo, W. Cao, J. Duan, H. Ni and C. Zhu, Water-Insoluble Organics Dominate Brown Carbon in Wintertime Urban Aerosol of China: Chemical Characteristics and Optical Properties, *Environ. Sci. Technol.*, 2020, **54**, 7836–7847.

28 R. Satish and N. Rastogi, On the use of brown carbon spectra as a tool to understand their broader composition and characteristics: a case study from crop-residue burning samples, *ACS Omega*, 2019, **4**, 1847–1853.

29 Y. Chen and T. Bond, Light absorption by organic carbon from wood combustion, *Atmos. Chem. Phys.*, 2010, **10**, 1773–1787.

30 N. J. Shetty, A. Pandey, S. Baker, W. M. Hao and R. K. Chakrabarty, Measuring light absorption by freshly emitted organic aerosols: optical artifacts in traditional solvent-extraction-based methods, *Atmos. Chem. Phys.*, 2019, **19**, 8817–8830.

31 M. Zheng, G. R. Cass, J. J. Schauer and E. S. Edgerton, Source apportionment of PM2. 5 in the southeastern United States using solvent-extractable organic compounds as tracers, *Environ. Sci. Technol.*, 2002, **36**, 2361–2371.

32 P. M. Fine, G. R. Cass and B. R. Simoneit, Chemical characterization of fine particle emissions from the fireplace combustion of woods grown in the southern United States, *Environ. Sci. Technol.*, 2002, **36**, 1442–1451.

33 D. A. Fischer and G. D. Smith, A portable, four-wavelength, single-cell photoacoustic spectrometer for ambient aerosol absorption, *Aerosol Sci. Technol.*, 2018, **52**, 393–406.

34 S. M. Phillips and G. D. Smith, Spectroscopic comparison of water-and methanol-soluble brown carbon particulate matter, *Aerosol Sci. Technol.*, 2017, **51**, 1113–1121.

35 J. P. Wong, M. Tsagkaraki, I. Tsiodra, N. Mihalopoulos, K. Violaki, M. Kanakidou, J. Sciare, A. Nenes and R. J. Weber, Atmospheric evolution of molecular-weight-separated brown carbon from biomass burning, *Atmos. Chem. Phys.*, 2019, **19**, 7319–7334.

36 C. Wu, X. Huang, W. M. Ng, S. M. Griffith and J. Z. Yu, Inter-comparison of NIOSH and IMPROVE protocols for OC and EC determination: implications for inter-protocol data conversion, *Atmos. Meas. Tech.*, 2016, **9**, 4547–4560.

37 B. Khan, M. D. Hays, C. Geron and J. Jetter, Differences in the OC/EC ratios that characterize ambient and source aerosols due to thermal-optical analysis, *Aerosol Sci. Technol.*, 2012, **46**, 127–137.

38 J. C. Corbin and M. Gysel-Beer, Detection of tar brown carbon with a single particle soot photometer (SP2), *Atmos. Chem. Phys.*, 2019, **19**, 15673–15690.

39 R. Subramanian, A. Y. Khlystov, J. C. Cabada and A. L. Robinson, Positive and negative artifacts in particulate organic carbon measurements with denuded and undenuded sampler configurations special issue of aerosol science and technology on findings from the fine particulate matter supersites program, *Aerosol Sci. Technol.*, 2004, **38**, 27–48.

40 H. S. El-Zanan, D. H. Lowenthal, B. Zielinska, J. C. Chow and N. Kumar, Determination of the organic aerosol mass to organic carbon ratio in IMPROVE samples, *Chemosphere*, 2005, **60**, 485–496.

41 A. C. Aiken, P. F. Decarlo, J. H. Kroll, D. R. Worsnop, J. A. Huffman, K. S. Docherty, I. M. Ulbrich, C. Mohr, J. R. Kimmel and D. Sueper, O/C and OM/OC ratios of primary, secondary, and ambient organic aerosols with high-resolution time-of-flight aerosol mass spectrometry, *Environ. Sci. Technol.*, 2008, **42**, 4478–4485.

42 L. Yao, L. Yang, J. Chen, X. Wang, L. Xue, W. Li, X. Sui, L. Wen, J. Chi and Y. Zhu, Characteristics of carbonaceous aerosols: Impact of biomass burning and secondary formation in summertime in a rural area of the North China Plain, *Sci. Total Environ.*, 2016, **557**, 520.

43 R. Chakrabarty, H. Moosmuller, L.-W. Chen, K. Lewis, W. Arnott, C. Mazzoleni, M. Dubey, C. Wold, W. Hao and S. Kreidenweis, Brown carbon in tar balls from smoldering

biomass combustion, *Atmos. Chem. Phys.*, 2010, **10**, 6363–6370.

44 D. A. Lack, J. M. Langridge, R. Bahreini, C. D. Cappa, A. M. Middlebrook and J. P. Schwarz, *Brown Carbon and Internal Mixing in Biomass Burning Particles*, Proceedings of the National Academy of Sciences, 2012.

45 T. C. Bond and R. W. Bergstrom, Light absorption by carbonaceous particles: An investigative review, *Aerosol Sci. Technol.*, 2006, **40**, 27–67.

46 D. Sengupta, V. Samburova, C. Bhattarai, E. Kirillova, L. Mazzoleni, M. Iaukea-Lum, A. Watts, H. Moosmüller and A. Khlystov, Light absorption by polar and non-polar aerosol compounds from laboratory biomass combustion, *Atmos. Chem. Phys.*, 2018, **18**, 10849–10867.

47 Z. Lu, D. G. Streets, E. Winijkul, F. Yan, Y. Chen, T. C. Bond, Y. Feng, M. K. Dubey, S. Liu and J. P. Pinto, Light absorption properties and radiative effects of primary organic aerosol emissions, *Environ. Sci. Technol.*, 2015, **49**, 4868–4877.

48 X. Li, Y. Chen and T. C. Bond, Light absorption of organic aerosol from pyrolysis of corn stalk, *Atmos. Environ.*, 2016, **144**, 249–256.

49 Y. Cheng, K.-b. He, Z.-y. Du, G. Engling, J.-m. Liu, Y.-l. Ma, M. Zheng and R. J. Weber, The characteristics of brown carbon aerosol during winter in Beijing, *Atmos. Environ.*, 2016, **127**, 355–364.

50 Y. Cheng, K.-b. He, G. Engling, R. Weber, J.-m. Liu, Z.-y. Du and S.-p. Dong, Brown and black carbon in Beijing aerosol: Implications for the effects of brown coating on light absorption by black carbon, *Sci. Total Environ.*, 2017, **599**, 1047–1055.

51 Y. Lei, Z. Shen, Q. Wang, T. Zhang, J. Cao, J. Sun, Q. Zhang, L. Wang, H. Xu and J. Tian, Optical characteristics and source apportionment of brown carbon in winter PM2. 5 over Yulin in Northern China, *Atmos. Res.*, 2018, **213**, 27–33.

52 G. Adler, N. L. Wagner, K. D. Lamb, K. M. Manfred, J. P. Schwarz, A. Franchin, A. M. Middlebrook, R. A. Washenfelder, C. C. Womack and R. J. Yokelson, Evidence in biomass burning smoke for a light-absorbing aerosol with properties intermediate between brown and black carbon, *Aerosol Sci. Technol.*, 2019, 1–33.

53 D. T. Alexander, P. A. Crozier and J. R. Anderson, Brown carbon spheres in East Asian outflow and their optical properties, *Science*, 2008, **321**, 833–836.

54 R. Stevens and A. Dastoor, A review of the representation of aerosol mixing state in atmospheric models, *Atmosphere*, 2019, **10**, 168.